

SMM DETECTION OF DIFFUSE GALACTIC 511 keV ANNIHILATION RADIATION

G. H. SHARE, R. L. KINZER, J. D. KURFESS, D. C. MESSINA,¹ AND W. R. PURCELL²
 E.O. Hulburt Center for Space Research, Naval Research Laboratory

E. L. CHUPP AND D. J. FORREST
 University of New Hampshire

AND

C. REPPIN

Max Planck Institute for Physics and Astrophysics, Institute for Extraterrestrial Physics, Garching

Received 1987 June 9; accepted 1987 September 1

ABSTRACT

The γ -ray spectrometer on NASA's *Solar Maximum Mission* satellite (*SMM*) has recorded a significant increase in the measured intensity of 511 keV line radiation in each of 5 yr as the Galactic center region passed through its 130° aperture. The overall statistical significance of the detection is in excess of 30 σ . Earth occultation and low-background data sets are utilized to demonstrate that this annual increase is due to a celestial source. Any year-to-year variation in the measured intensity is less than 30%. The time-averaged flux, if attributed to a point source at the Galactic center, is $(2.1 \pm 0.4) \times 10^{-3} \gamma \text{ cm}^{-2} \text{ s}^{-1}$, where the error is dominated by systematic uncertainties. However, comparison of this *SMM* flux, for an assumed point source at the Galactic center, with upper limits obtained with narrow aperture (15° FWHM) germanium spectrometers during contemporaneous balloon flights in 1981 and 1984 suggests that a bulk of the radiation observed by *SMM* comes from an extended region. If the 511 keV emission is proportional to the measured CO distribution in the Galaxy, then the inferred flux from the *SMM* observations is $(1.6 \pm 0.3) \times 10^{-3} \gamma \text{ cm}^{-2} \text{ s}^{-1} \text{ rad}^{-1}$ at the center. Possible contributors to an interstellar concentration of positrons include β -unstable nuclei (e.g., ⁵⁶Co, ⁴⁴Ti, ²⁶Al, ²²Na) produced in supernovae, novae, red giants, and Wolf-Rayet stars; cosmic-ray interactions with the interstellar medium; pulsars; black holes; and stellar flares. The presence of such a diffuse source accounts for much of the 511 keV radiation detected from the Galactic center region during balloon flights in the 1970s and is also consistent with the upper limits obtained in the 1980s. The presence of this diffuse source also weakens the evidence for a variable source at the Galactic center.

Subject headings: galaxies: The Galaxy — galaxies: nuclei — gamma rays: general — nucleosynthesis — radiation mechanisms

I. INTRODUCTION

Positrons can be produced as by-products of nucleosynthesis and nuclear interactions in astrophysical sites as diverse as supernovae and the interstellar medium. The 0.511 MeV γ -ray line, which results from the annihilation of positrons, has been studied in Earth's atmosphere (Mahoney, Ling, and Jacobson 1981) and solar flares (Share *et al.* 1983). It is also the first celestial γ -ray line to be detected.

Celestial annihilation line measurements were pioneered by the group at Rice University in the late 1960s and early 1970s (Johnson and Haymes 1973; Haymes *et al.* 1975) using a balloon-borne experiment containing a collimated NaI detector. Four observations were conducted in 1968, 1970, 1971, and 1974. A line feature near 0.5 MeV appeared above the background from the region of the Galactic center in each of these observations. However, uncertainties in the line's energy prevented it from being identified with positron annihilation without ambiguity. This feature, if interpreted as a point source, had a measured intensity of $(1.8 \pm 0.5) \times 10^{-3} \gamma \text{ cm}^{-2} \text{ s}^{-1}$ from the combined 1970 and 1971 exposures, but dropped to $(0.80 \pm 0.23) \times 10^{-3} \gamma \text{ cm}^{-2} \text{ s}^{-1}$ in 1974. This reduction in intensity was interpreted as either evidence for an extended

source (the 1974 instrument had an aperture of 13° FWHM in contrast to 24° FWHM for the earlier instrument) or for source variability.

The ambiguity in identification of this Galactic line was resolved in 1977 November by the Bell/Sandia Laboratories' balloon-borne germanium spectrometer having a 15° (FWHM) aperture (Leventhal, MacCallum, and Stang 1978). This group reported detection of a line centered at 510.7 ± 0.5 keV with a flux of $(1.22 \pm 0.22) \times 10^{-3} \gamma \text{ cm}^{-2} \text{ s}^{-1}$ when the instrument was pointed at the Galactic center. Leventhal *et al.* (1980) reported confirmation of this detection based on analysis of data from a subsequent balloon flight with the same instrument in 1979.

Measurements of the Galactic 511 keV line were also reported based on analysis of data from two other balloon-borne spectrometers flown in 1977. The Centre d'Etude Spatiale des Rayonnements (CESR), Toulouse, flew a germanium spectrometer with an aperture of about 50° FWHM in 1977 February. Albernhe *et al.* (1981) used two different methods of analysis which suggested the presence of a line from the vicinity of the Galactic center with an intensity of either (4.2 ± 1.6) or $(3.4 \pm 2.1) \times 10^{-3} \gamma \text{ cm}^{-2} \text{ s}^{-1}$, depending on the method, for an assumed point source. The apparently high flux relative to earlier observations lead these authors to conclude that the measured intensity was dependent on instrument aperture, suggesting that the source is extended.

¹ Also Sachs/Freeman Assoc., Inc.

² Also Northwestern University.

The University of New Hampshire's balloon-borne NaI experiment, with an aperture of about 100° FWHM, detected an excess flux of about $4.0 \times 10^{-3} \gamma \text{ cm}^{-2} \text{ s}^{-1}$ from the general vicinity of the Galactic center in 1977 (Gardner *et al.* 1982); their estimate of the line flux is dependent on the fraction of annihilations occurring through the production of positronium. For a positronium fraction of 90%, the inferred line flux from a point source is about $3.2 \times 10^{-3} \gamma \text{ cm}^{-2} \text{ s}^{-1}$. This flux is about a factor of about 3 higher than what was measured 10 days earlier by Leventhal, MacCallum, and Stang (1978). Gardner *et al.* suggest that this difference may be attributed to source variability, narrow and broad line components, and/or extended emission from the Galactic plane.

Striking evidence for variability of a Galactic center source was presented by Riegler *et al.* (1981) based on data obtained from the *HEAO 3* germanium spectrometer. Analysis of data from a 1979 autumn exposure exhibited a narrow 511 keV line with an intensity of $(1.85 \pm 0.21) \times 10^{-3} \gamma \text{ cm}^{-2} \text{ s}^{-1}$, while analysis of data accumulated in a 1980 spring exposure indicated that the intensity of the line had dropped to $(0.65 \pm 0.27) \times 10^{-3} \gamma \text{ cm}^{-2} \text{ s}^{-1}$. Riegler *et al.* concluded that the spatial distribution of the radiation measured with *HEAO 3*'s 35° FWHM aperture ruled out extended sources of positron production, such as multiple supernovae, and that the 511 keV line most likely originated in a single compact source at the Galactic center.

Analysis of data from subsequent flights of the Bell/Sandia spectrometer in 1981 and 1984 (Leventhal *et al.* 1986) indicated a sharp decline in the Galactic center annihilation line intensity relative to their earlier detections in 1977 and 1979. Upper limits of $1.0 \times 10^{-3} \gamma \text{ cm}^{-2} \text{ s}^{-1}$ with 98% confidence were set on the flux from the source during the latter observations. A NASA Goddard Spaceflight Center/Centre d'Etudes Nucleaires de Saclay balloon-borne experiment with a germanium spectrometer (15° FWHM aperture) was conducted in 1981, within a day of the observation by Leventhal *et al.*, and set a comparable 98% confidence limit of $1.2 \times 10^{-3} \gamma \text{ cm}^{-2} \text{ s}^{-1}$ on the source intensity (Paciesas *et al.* 1982).

Dunphy, Chupp, and Forrest (1983) reviewed most of the 511 keV measurements and concluded that the ensemble are consistent with the presence of both a time-varying point source and an extended Galactic source. However, they also pointed out that some of the disparate source intensities could have resulted from systematic errors in the measurements, such as the technique used to correct for background.

In this paper we present observations of the 511 keV annihilation line from the vicinity of the Galactic center from October to February for 1980/1981, 1981/1982, 1982/1983, 1984/1985, 1985/1986. These measurements were made with the gamma-ray spectrometer (GRS) on NASA's *Solar Maximum Mission* satellite (*SMM*). Although it was designed for solar studies, the spectrometer's excellent stability, good sensitivity, and long observing period have allowed its use in observations of Galactic γ -ray lines. The measurement of the 1.81 MeV line from the decay of ^{26}Al in the interstellar medium (Share *et al.* 1985) is an example of this capability. In § II we describe the design of the instrument and some of its properties which have been used in the analysis. The methods used for accumulating, fitting, and analyzing the data are outlined in § III. We discuss the results of this analysis in § IV and describe how we are able to separate the Galactic 511 keV line from the intense and variable background observed in orbit. In § V we summarize the results of this analysis, compare the *SMM*

observations with previous measurements of annihilation radiation from the Galactic center region, and discuss the astrophysical implications. We argue that most of the measurements made to date suggest the presence of an extended Galactic source of annihilation radiation. Preliminary reports of these *SMM* measurements have appeared previously (Share *et al.* 1986, 1987).

II. INSTRUMENT DESCRIPTION

The *Solar Maximum Mission* satellite was launched on 1980 February 14 with a complement of seven experiments to observe the Sun during the peak of 11 year cycle 21. A problem developed with the satellite's attitude control system in the latter part of 1980. This problem had only a small effect on observations made by the Gamma-Ray Spectrometer (GRS). The spacecraft's attitude control system was repaired by the Shuttle astronauts in 1984 April, and the satellite is still operating normally. Data have been collected almost continuously by the GRS since launch, with the exception of a 5 month period prior to the repair when the satellite's tape recorders were turned off.

The GRS consists of seven $3'' \times 3''$ NaI detectors in a close-packed array enclosed in a 4π sr anticoincidence shield (see Fig. 1). The spectrometer has a broad field of view for γ -radiation, defined by a $1''$ thick CsI annulus around the sides of the detectors and a $3''$ thick CsI anticoincidence disk behind the NaI detectors. A plastic scintillation counter covers the forward aperture and rear of the detector to complete the 4π sr charged-particle shield. The spectrometer is sensitive to γ -rays between 300 keV and 8.5 MeV, with an energy resolution at 511 keV of 8%, or 41 keV FWHM. It has an effective area of 150 cm^2 for detecting a line at 511 keV. A 476 channel energy spectrum is accumulated every 16.38 s. A detailed description of the GRS is presented in Forrest *et al.* (1980).

Knowledge of the angular response of the instrument is an important element in the study of celestial emissions. Unfortunately, no angular calibrations were performed prior to launch of the satellite. In lieu of a calibration we have utilized a Monte Carlo simulation (Jung and Matz 1987) to estimate this response. The GRS angular response function derived from this analysis is shown in Figure 2 and indicates that the instrument has a field of view of $\sim 130^\circ$ FWHM at 511 keV.

The excellent gain stabilization of the GRS has been an essential element in the long-term measurements of line intensities that is fundamental to making celestial γ -ray observations. This stability is exhibited in Figure 3 which displays the count-rate spectrum accumulated from launch through 1986 September, outside of orbits traversing the high-radiation zones of the South Atlantic Anomaly (SAA), and with the GRS pointed away from Earth. Three of the most prominent lines in this spectrum are due to the on-board ^{60}Co calibration source; these lines are at 1.17, 1.33, and 2.50 MeV (sum peak). The apparent peak-to-valley ratio for the 1.17 and 1.33 MeV lines is reduced due to the build-up of the 1.275 MeV instrumental background line from ^{22}Na ($\tau_{1/2} = 2.6$ yr). There has been no observable degradation in the spectrometer's resolution since prelaunch calibrations in 1979.

Most of the continuum and line features displayed in Figure 3 below about 3 MeV are due to radioactive products in the detector and surrounding materials from irradiation by particles in the Van Allen belts (SAA) and by cosmic rays. Many of these lines are blended. Possible identifications of these radioactive features are $\sim 390 \text{ keV}$ (^{113}Sn , ^{126}I , ^{127}Xe , ^{129}Cs); ~ 460

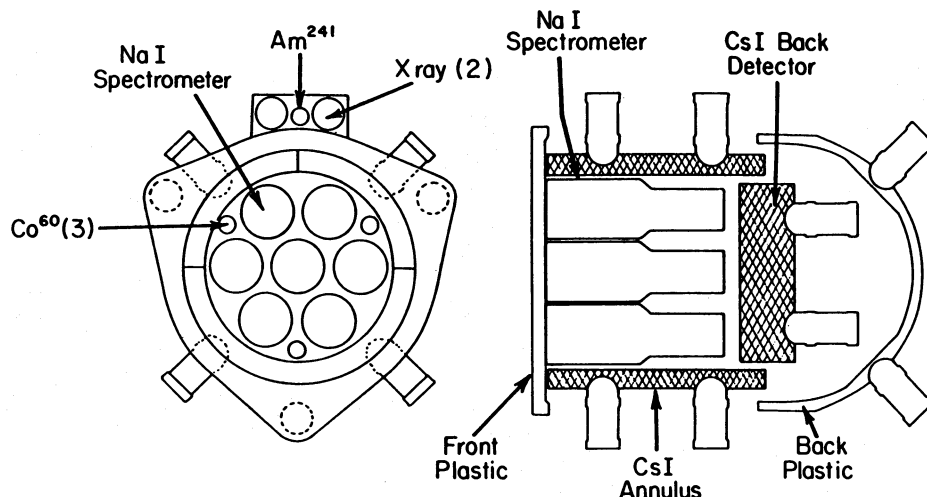


FIG. 1.—Schematic drawing of the Gamma-Ray Spectrometer (GRS) experiment on *SMM*

keV (^{132}Cs); ~ 511 keV (^{22}Na , ^{121}Te , ^{132}Cs); ~ 610 keV (^{121}Te , ^{124}I); 630–700 keV (^{119}Te , ^{126}I , ^{132}Cs); ~ 820 keV (^{54}Mn , ^{58}Co); ~ 1.4 MeV (^{24}Na , ^{40}K); ~ 1.8 MeV (^{22}Na , ^{26}Mg , ^{28}Si , ^{119}Te); 2.75 MeV (^{24}Na). Leakage of atmospheric γ -ray lines (e.g., 511 keV) also contributes to the background spectrum. Letaw *et al.* (1986, 1987) have identified at least 20 line features in the atmospheric spectrum using *SMM*.

III. DATA ANALYSIS

a) Data Base

The GRS accumulates a 476 channel spectrum from ~ 300 keV to ~ 8.50 MeV in each consecutive 16.384 s interval. These spectra were processed and summed into 1 minute accumulations which form the data base for this analysis. Each 1 minute spectrum was examined for data quality. Only high-quality data not associated in time with known solar flares, cosmic γ -ray bursts, or terrestrial background events were included in this analysis. These screened data were then further summed

over 3 day intervals into 1000 spectra determined by three background parameters. Each parameter has 10 binning ranges, so that each of the 1000 spectra corresponds to a unique combination of background parameters.

The first of these parameters is the time from the last traversal of the SAA. During transits of the SAA, irradiation by intense fluxes of protons and neutrons activate detector and spacecraft materials, producing increased line and continuum rates which return to nominal background levels within a few hours after SAA traversals. For example, the intensity of the 511 keV line following such a traversal can increase by a factor of 10 above its nominal level. In order to minimize background in our celestial studies, we exclude data from orbits containing an SAA traversal. The remaining “SAA-free” time is broken up into 10 ~ 70 m accumulation intervals. Analysis based on this time parameter permits selection of data which are least affected by the SAA irradiations and assists in understanding how the SAA irradiations affect the measurement of celestial γ -rays.

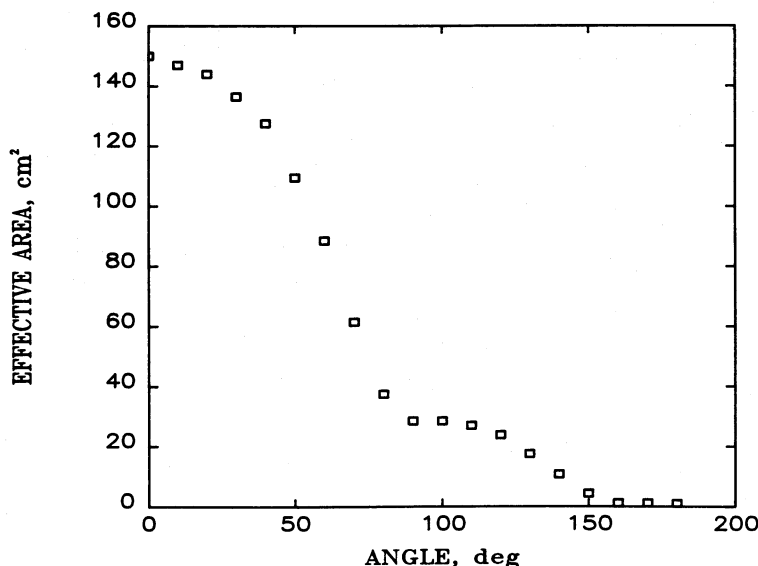


FIG. 2.—Estimated efficiency of the GRS to incident 511 keV photons as a function of angle derived from a Monte Carlo simulation of the instrument

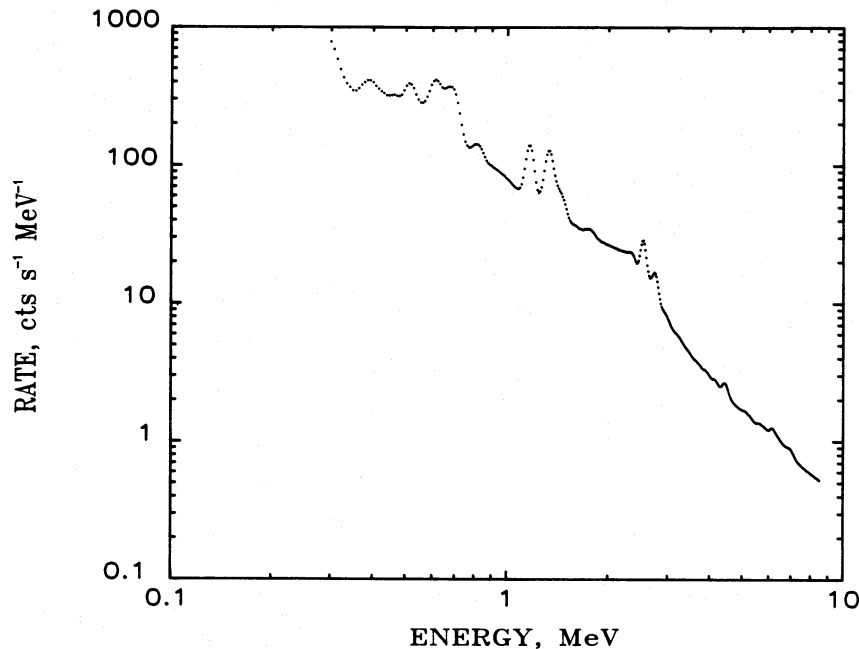


FIG. 3.—Overall background spectrum accumulated by the GRS $>10^4$ s from the last traversal of the radiation belts (SAA), for magnetic cutoff rigidities >4 GV, and with the instrument's aperture pointing $>108^\circ$ from the center of Earth. This spectrum was accumulated over a total of 2×10^7 s from launch in 1980 February through 1986 November. Statistical uncertainties are smaller than the plotted data points.

The second parameter is the angle of the detector axis relative to the center of Earth (“Earth-angle”). Because *SMM* is solar oriented, this angle varies with an ~ 95 minute period. This angle parameter measures the exposure to atmospheric γ -rays and has been divided into 10 bins of 36° width. Selection of spectra based on “Earth-angle” permits effects of atmospheric γ -rays to be minimized and also facilitates the use of Earth as an occulter for extraterrestrial sources.

Vertical geomagnetic cutoff rigidity is the third binning parameter. This parameter is useful in understanding the influence of cosmic radiation and the atmospheric background radiation on the measured spectra. The 10 ranges of rigidity which were selected to produce approximately equal live times in each bin, are <5 , $5-7$, $7-8.5$, $8.5-10$, $10-11$, $11-12$, $12-13$, $13-14$, $14-15$, and >15 GV.

By summing selected sets of bins, we obtain 3 day spectra which were accumulated over a particular range of each parameter. In our ensuing analysis we shall utilize only spectral data accumulated more than $\sim 10^4$ s from the last traversal of the SAA, in order to reduce the radioactive background. We also make use of both the total range in magnetic rigidity and a subset covering the range above 11 GV, in order to demonstrate that our results are independent of cosmic-ray intensity. In the next section we describe how the Earth-angle is used to discriminate between a true celestial source and background.

b) Detecting a Galactic Source of γ -Rays with *SMM*

We use the fact that the *SMM*/GRS detection axis follows the sun along the ecliptic to search for an annual increase of annihilation line photons as the Galactic center passes through its field of view. The Sun crosses the Galactic equator within 6° of the center in the latter part of December. Because of the GRS's large aperture ($\sim 130^\circ$ FWHM at 511 keV), sources in the vicinity of the Galactic center are observable for up to 4–5 months each year. Failures in *SMM*'s attitude control system

in 1980 November, which resulted in up to an $\sim 11^\circ$ uncertainty in pointing, did not seriously impact this analysis. *SMM* was repaired by the Shuttle astronauts in 1984 April.

A schematic illustration of how the *SMM*/GRS detects a celestial source of γ -radiation is displayed in Figure 4. In this representation Earth and satellite are viewed from above the north pole. *SMM* moves around Earth in a counterclockwise direction. We display the four broad viewing geometries relative to Earth which we have used in this report: “sky viewing”—*SMM* near satellite noon ($\theta > 108^\circ$, where θ is the angle between the detector axis and center of Earth as viewed from *SMM*); “Earth viewing”—*SMM* near satellite midnight ($\theta < 72^\circ$); and “partially occulted”—*SMM* near the day/night or night/day terminators ($72^\circ < \theta < 108^\circ$). A celestial source moves relative to the Sun in a clockwise direction. We plot pictorial representations of the instrument's response to a transiting celestial source below each of the four viewing positions. The response for the “sky-viewing” position mirrors the off-axis sensitivity of the GRS. Earth occultation plays a large role in the response of the GRS for the other viewing geometries.

We briefly discuss the GRS's response to a celestial source observed in the “Earth-viewing” and “partially occulted” configurations. The response plotted under the “Earth-viewing” configuration exhibits (1) an increase as the source enters the GRS field of view, (2) a decrease as the source moves behind Earth, (3) an increase as the source reappears behind Earth, and (4) a decrease as it leaves the field of view. This time history is an approximation because it assumes that the source, the Sun, and *SMM*'s orbit are all coplanar. A detailed time history for most sources will exhibit more structure due to *SMM*'s orbital inclination and precession.

When *SMM* views the transit of a source from its “partially occulted” geometry, the time history will appear asymmetric, as illustrated in Figure 4. With *SMM* near its night/day transition, the source is occulted for the early part of the transit;

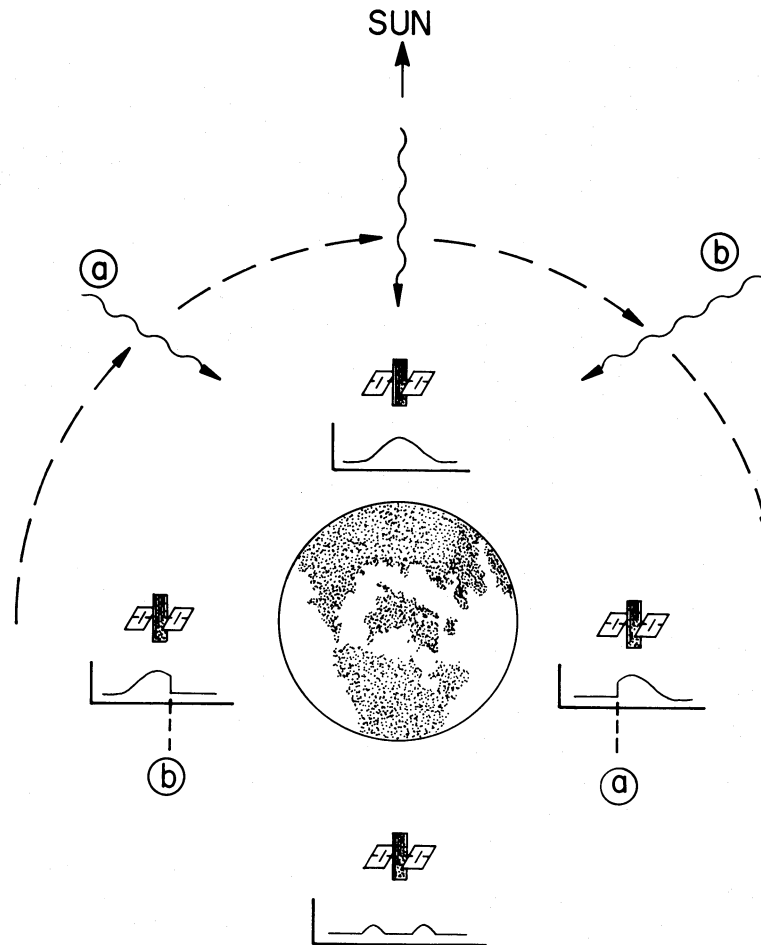


FIG. 4.—Schematic representation of the transit of a celestial source through the *SMM/GRS* aperture illustrating the effects of occultation by the earth. Four representative viewing geometries relative to Earth are shown: “sky-viewing,” $\theta > 108^\circ$; “partially occulted,” $72^\circ < \theta < 108^\circ$; “earth-viewing,” $\theta < 72^\circ$ (where θ is the angle between the Sun and center of Earth as measured from *SMM*). Source locations (a) and (b) illustrate partial occultation by Earth. A simplified time profile for the detection of a celestial source is displayed below each geometry.

the reverse is true for the day/night transition. Labels (a) and (b) denote the times when the source appears above the edge of Earth or disappears below the edge of Earth, respectively, for a specific orbital position. Note that once again the illustrated time histories do not take into account orbital precession.

The ability to demonstrate that the time history of the annihilation line detected by *SMM* is consistent with occultation of a Galactic source is a critical element in confirming its celestial origin. This will be discussed in § IVd below.

c) Spectral Fits

The spectral region near 0.511 MeV contains a number of background lines (see Fig. 3 and our earlier discussion). In this section we describe the methods we have used to isolate our measurement of the annihilation line from these nearby background features and explain the observed temporal variations.

An expanded view of the count-rate spectrum from 350 to 760 keV for “sky-viewing” data accumulated over a 3 day interval is shown in Figure 5. At least five line features are evident. It is likely that most of these contain blends of more than one individual line. We suggested some identifications for these features in § II. Our ability to identify the specific radioactive lines is aided by observing the temporal evolution of

both the feature’s energy, width, and intensity over the 7 yr lifetime of the mission. In order to do this we have assumed that the spectral data in this energy range can be described by five gaussian lines superposed over a continuum which is represented by a quadratic function. The solid curve in Figure 5 is the best fit to the data using this model. This model is only a fair representation of these data of statistically high significance because the fits typically produce a χ^2/DOF (degree of freedom) of no less than ~ 6 for a given 3 day summed spectrum.

A second spectral analysis has been used to confirm our detection of the Galactic 511 keV flux. This method uses a “difference” spectrum in order to demonstrate that our results are independent of the fitting procedure. Most of the radioactive background features in the “sky-viewing” spectrum shown in Figure 5 can be eliminated by a process of subtraction. We have accomplished this by subtracting “sky-viewing” data from “Earth-viewing” data (see Fig. 4). This has the effect of producing a spectrum which is dominated by atmospheric γ -radiation; any celestial γ -ray line will appear as a negative feature in this spectrum. This differencing technique has been used to measure the γ -ray spectrum of the atmosphere (Letaw *et al.* 1986, 1987) and to set limits on any Doppler-shifted line

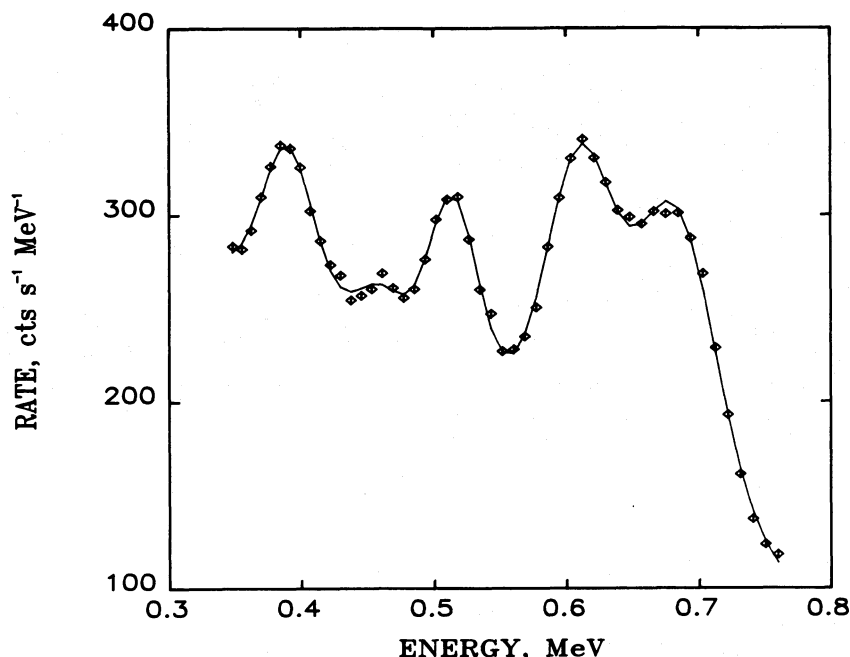


FIG. 5.—Count-rate spectrum obtained during a 3 day observation period with the GRS viewing the sky. Included are data accumulated at magnetic rigidities ≥ 4 GV and at times in excess of $\sim 10^4$ s from the last transit of the SAA. The solid curve is the best-fit model consisting of five Gaussian-shaped lines superposed above a continuum represented by a quadratic function. The statistical uncertainties are about the size of the data points.

emission from SS 433 (Geldzahler *et al.* 1985). A plot of this count rate spectrum covering the energy range near 511 keV is shown in Figure 6. This spectrum primarily contains contributions from a narrow line at 511 keV and its Compton-scattered continuum. Therefore a very different set of fitting parameters is used to obtain the 511 keV time history. We use the results of this fit in § IVd to confirm our detection of a Galactic 511 keV flux.

IV. RESULTS

a) Background Variations

Plotted in Figure 7 are the measured intensities for six of the parameters obtained from the fit to the “sky-viewing” spectrum (i.e., Fig. 5) covering the period from within 15 days of launch (1980 February) to the summer of 1986. The data are plotted at 3 day resolution. Striking variations are apparent in

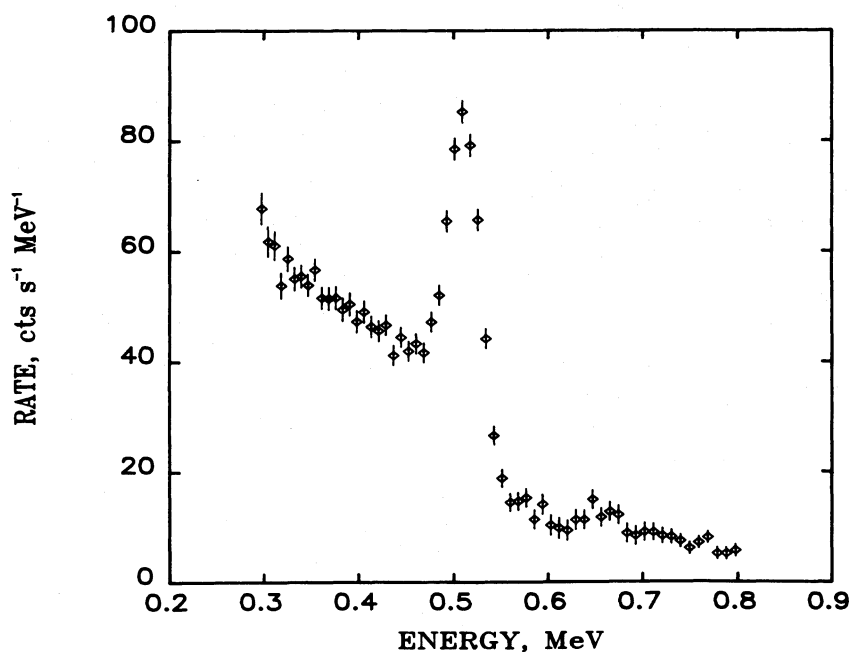


FIG. 6.—Count-rate spectrum obtained after subtracting “sky-viewing” data from “Earth-viewing” data accumulated over the same 3 day period. Radioactively produced features are subtracted, revealing the γ -ray spectrum emitted by Earth’s atmosphere. Any celestial lines will appear as negative features in this representation.

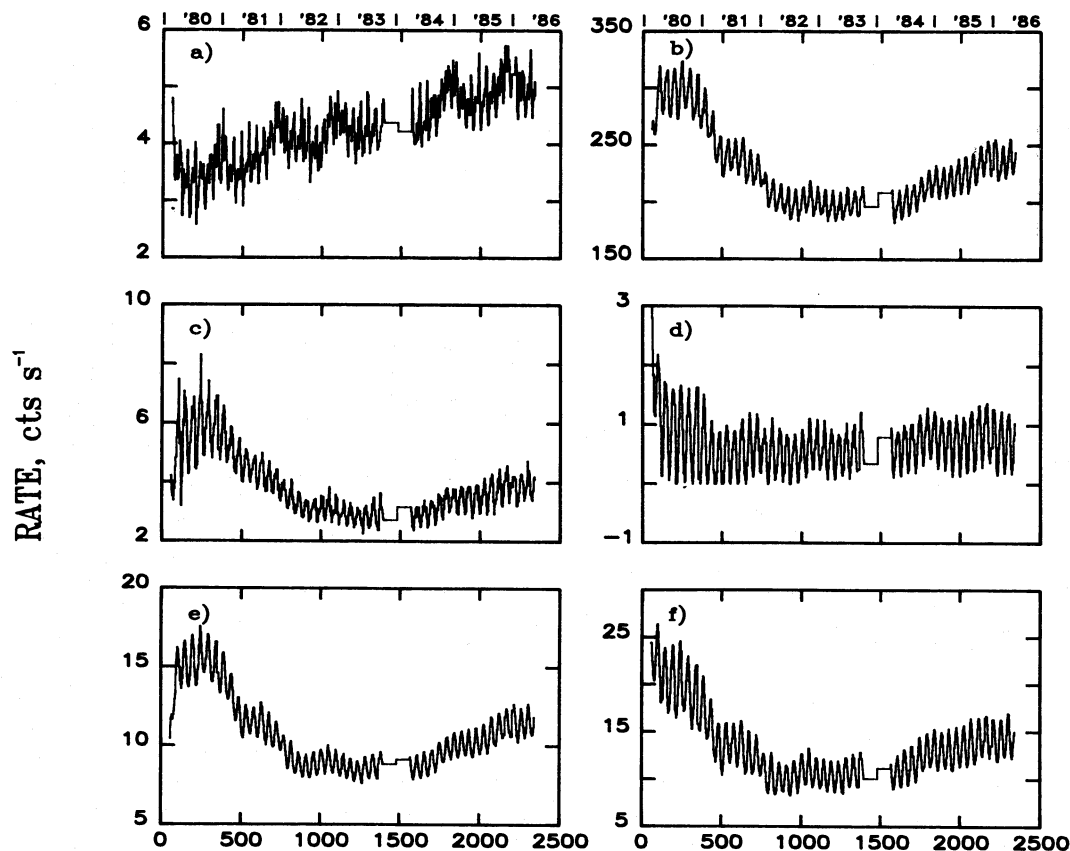


FIG. 7.—Time variations of the measured intensities of six of the parameters used to fit the “sky-viewing” count-rate spectrum exhibited in Fig. 5. Time resolution is 3 days. Statistical are too small to be resolved. (a) ~ 511 keV feature, (b) first term in quadratic expression for underlying continuum, (c) ~ 390 keV feature, (d) ~ 460 keV feature, (e) ~ 610 keV feature, (f) ~ 680 keV feature. *SMM*'s tape recorder was turned off from 1983 November until its repair in 1984 April causing the observed data gap.

some lines within the first few days of the mission due to the rapidly changing background and, to some degree, changing operating modes of the satellite. The time histories of all the intensities, except for the feature near 511 keV, are similar. They all exhibit an ~ 47 day period (this period has changed from about 48.2 days to about 46.5 days over the lifetime of *SMM*), the orbital precession period relative to the Sun, superposed on similar long-term trends. The ~ 47 day period reflects the irradiation of the GRS by particles in the radiation belts (SAA), while the long-term trend reflects SAA and cosmic-ray irradiations.

The ~ 47 day period is due to a combination of the anisotropy of particles in the SAA, the solar orientation of *SMM*, and precession of its orbit. Every ~ 47 days the GRS traverses the SAA in an orientation such that the particle irradiation of the instrument is a maximum. This orientation occurs near the time when *SMM* is about to enter the nighttime portion of its orbit. The amplitude of the 47 day modulation also appears to be proportional to the intensity of the long-term variation, suggesting that the long-term variation is primarily caused by particles in the SAA.

The long-term variations are determined, in part, by the half-lives of the specific radioactive isotopes that are produced. For example, features plotted in Figures 7b, 7c, and 7e exhibit a more gradual initial build-up in intensity than that plotted in Figure 7f. All of the features, with the exception of the 511 keV

line, exhibit a decrease in intensity until about 800 days after launch. This decrease is attributed to the reduced exposure to particles in the SAA because the altitude of *SMM* dropped from about 575 km to about 510 km during that time interval. The long-term intensity begins to rise about 1500 days following launch (1984 spring) even though the altitude of *SMM* dropped an additional 10 km by the autumn of 1986. We attribute this rise to the approach of solar minimum. During solar minimum two effects occur that could increase the particle irradiation of the GRS: (1) The density of the upper atmosphere decreases resulting in an increase in the equilibrium intensity of the particles in the radiation belts; and (2) the cosmic-ray intensity increases with the decrease in solar modulation. As mentioned above, because the amplitude of the 47 day modulation also increases after 1984, we believe that most of the induced radioactivity in the instrument is produced by particles in the radiation belts.

Differences in the intensity histories plotted in Figure 7 assist in the identification of the isotopes responsible for the line features. For example, the feature near 680 keV (Fig. 7e) appears to fall in intensity soon after launch, whereas the feature near 390 keV (Fig. 7c) appears to be building up for the first 100 days or so. This suggests that the 680 keV feature is produced by an isotope with a half-life of a few days or less, whereas the feature near 390 keV is produced by an isotope with a half-life of ~ 100 days. For this reason we infer that

^{113}Sn ($\tau_{1/2} = 115$ days, $E_\gamma = 391.7$ keV) is a large contributor to the 390 keV feature.

Another feature which builds up on the order of tens of days is the one near 610 keV. A possible isotope which contributes to this feature is ^{121}Te ($\tau_{1/2} = 16.78$ days). This isotope produces a line in NaI at 604.9 keV (573.1 keV plus K -shell X-ray of 31.8 keV). It also produces a line at 539.4 keV in NaI. A spectrum created by subtracting data near launch from those obtained ~ 60 days after launch exhibits such a feature near 540 keV. Additional evidence for this line comes from fits made to the 511 keV feature. We find that its energy appears to increase in the early stages of the mission from ~ 511 keV up to ~ 514 keV, indicating the presence of a higher energy line which increases in intensity. Another possible contributor to the 511 keV feature is a line at 505.8 keV from ^{132}Cs , which also produces line observable lines at 464 and 668 keV.

b) Temporal Variation of 511 keV Feature

The primary contributor to the background features near 511 keV is annihilation radiation from both within the instrument and from the earth's atmosphere. The time history of this feature, displayed in Figure 7a for the "sky-viewing" data, exhibits both a long-term increase and periodic variations. The long-term increase contrasts with the profiles observed in the other line features and continuum obtained from the same fit to the 350 to 760 keV spectrum (Fig. 5). This increase is due to the build-up of ^{22}Na (β^+ emitter; $\tau_{1/2} = 2.6$ yr), a spallation product of aluminum in the detector housing. The build-up of the 1.275 MeV radioactive decay line from ^{22}Na has also been observed in the GRS during a search for line emission at this energy from novae (Leising *et al.* 1988). In addition, the sum

peak from coincident detection of both the 1.275 and 0.511 MeV γ -rays has also been observed (Share *et al.* 1985).

Superposed on the long-term increase in the annihilation line are short-term structures. An expanded plot of the data in Figure 7a reveals both ~ 24 and ~ 47 day periodicities. We attribute the ~ 47 day periodicity to the presence of blended radioactive lines such as ^{132}Cs and ^{121}Te (see above discussion). We attribute the ~ 24 day periodicity to leakage of atmospheric 511 keV photons through the anticoincidence shield and to unstable isotopes with $\tau_{1/2} \gtrsim 1$ minutes produced by cosmic radiation, and emitting either positrons or line γ -rays near 511 keV.

This ~ 24 day periodicity can be explained by the precession of *SMM*'s orbit. For example, if one follows the latitude of *SMM* when it is near the night/day terminator, one finds that it will vary from $+28^\circ$ to -28° and back again in ~ 47 days. Thus, with respect to magnetic rigidity, *SMM* moves through two full cycles in ~ 47 days at any given "Earth-angle". This means that cosmic-ray-induced atmospheric and detector backgrounds will exhibit an ~ 24 day periodicity. Because the dipole magnetic field is offset from the center of Earth, the average rigidity at positive geographic latitudes is different from that at negative latitudes. For example, the average vertical cutoff rigidity at 400 km and at $+30^\circ$ latitude is about 9.6 GV as compared with about 7.3 GV at -30° (Humble, Smart, and Shea 1979). This will produce a periodic variation with alternating high and low peaks. An expanded view of the 511 keV profile observed by *SMM* near its night/day terminator from late 1984 to early 1986 is plotted in Figure 8a. The periodicity is obvious when the detector is in this geometry (i.e., "Earth-angle" $\approx 90^\circ$) because the 511 keV intensity profile is dominated by the atmospheric line. We also note that the peak

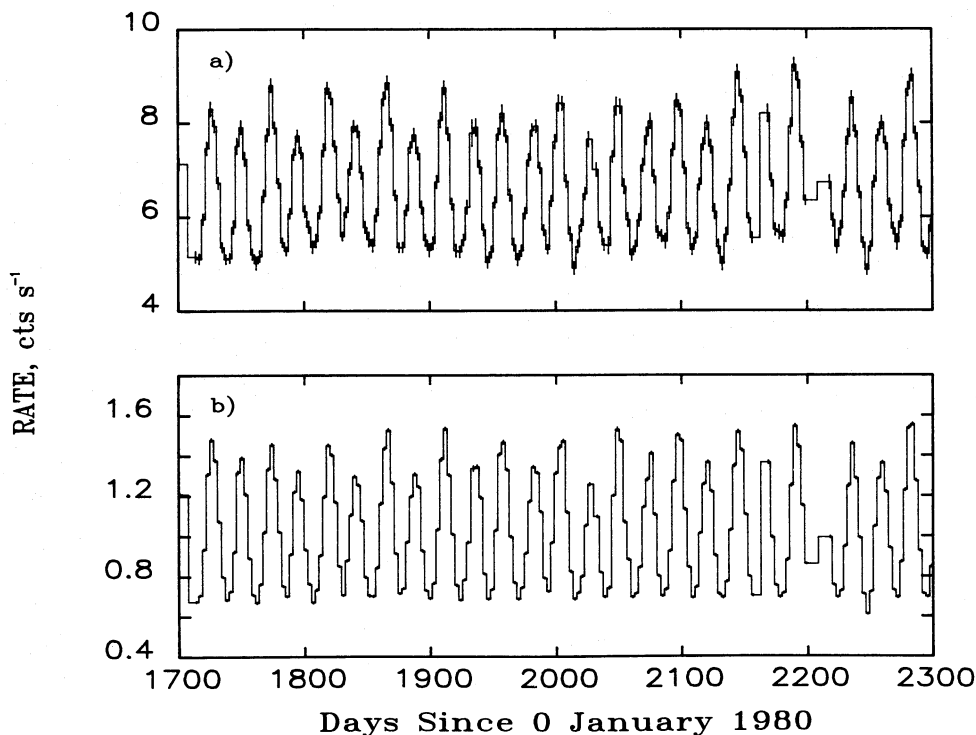


FIG. 8.—Expanded view of intensity variations observed from late 1984 to early 1986 with *SMM* near Earth's night/day terminator. (a) 511 keV feature, (b) integral rate observed between 5 and 8.5 MeV.

intensities alternate between high and low values, as expected from our discussion above.

The 511 keV intensity profile also exhibits a significant variation not found in any of the other intensities plotted in Figure 7. A peak in the 511 keV intensity is evident in the latter part of each year. The amplitude of this modulation is ~ 0.5 counts s^{-1} or about 12% of the average rate observed in the line feature. This peaking in intensity is coincident with the transit of the Galactic center through the GRS's broad aperture. In the next section we discuss the methods used to improve the quality of 511 keV line measurements by removing various background contributions.

c) Correcting the 511 keV Intensities for Background

The observed 511 keV line intensities plotted in Figure 7a contain contributions from radioactive isotopes produced within the instrument and spacecraft, and from Earth-albedo which leaks into the detector, in addition to any celestial radiation. Radioactive lines, such as those from ^{132}Cs (505.8 keV, $\tau_{1/2} = 6.47$ days) and ^{121}Te (539.4 keV, $\tau_{1/2} = 16.8$ days), cannot be resolved from the annihilation line. They produce long-term and ~ 47 day temporal variations in the 511 keV feature which are expected to be similar to those shown in Figures 7e and 7f.

On the other hand, leakage 511 keV γ -rays from the atmosphere and from locally produced positron emitters with $\tau_{1/2} \gtrsim 1$ minute are expected to follow variations of atmospheric albedo γ -rays produced by the local cosmic radiation. These albedo γ -rays consist of both a bremsstrahlung continuum and lines from excited states of atmospheric nuclei (Letaw *et al.* 1986, 1987). We use the integral rate observed in the GRS between 5 and 8.5 MeV, which includes both Earth albedo bremsstrahlung and nuclear lines but only a small contribution from radioactive isotopes, as a monitor of the intensity of 511 keV photons from Earth albedo. Plotted in Figure 8b is an expanded view of the temporal variation of the integral 5 to 8.5 MeV rate from late 1984 to early 1986 for data accumulated near the night/day terminator. The ~ 24 day periodic variation of the integral 5–8.5 MeV rate closely follows the 511 keV line intensity plotted in Figure 8a. Thus time variations in the integral 5–8.5 MeV rate provide a monitor of the intensity variations of the 511 keV line produced by cosmic radiation.

We have therefore used the measured temporal variations of the ~ 680 keV line intensity (Fig. 7f) and the integral 5–8.5 MeV intensity to remove the ~ 24 and ~ 47 day modulations which appear in the 511 keV time profile for the “sky-viewing” data shown in Figure 7a, as well as for other viewing geometries. This was done by fitting the 511 keV time profile with a model which includes (1) a cubic function to approximate the long-term build up due to ^{22}Na , (2) the 680 keV time profile multiplied by a constant, (3) the 5–8.5 MeV intensity multiplied by a constant, and (4) the calculated shape of the annual transit of a Galactic center source through the GRS's aperture (see discussion below) multiplied by a constant. The best values for the parameters defined above were determined by a least-squares fit to the 511 keV intensity profile for the given viewing geometry. (In order to remove any zero offset from the corrected 511 keV profile, the 5–8.5 MeV intensity profile was first normalized so that its time-averaged value was 0.) Using the best-fit parameters we were able to significantly reduce the ~ 24 and ~ 47 day periodicities observed in the 511 keV intensity profile. The shape of the long-term increase was also modi-

fied because both the radioactive and atmospheric components vary over the solar cycle.

A brief explanation of how the errors in the 511 keV line intensities were determined is appropriate here. As we discussed earlier (§ IIIc), these intensities were derived by fitting 3 day spectral accumulations with a model containing five Gaussian lines superimposed on a quadratic continuum. This relatively simple model typically produced fits with $\chi^2/\text{DOF} \approx 6$; therefore, the algorithm arbitrarily increased the errors on the 511 keV intensities in order to compensate for the relatively poor fit. We have found that the errors derived for the “sky-viewing” data were larger than the measured fluctuations in intensity. We therefore scaled down the size of the errors for the “sky-viewing” 511 keV intensities until a simple quadratic function could fit the background intervals outside of the Galactic transits with a χ^2/DOF of ~ 1 . This scaling was not applied to the “Earth-viewing” data because of the larger systematic variations caused by the dominant presence of the atmospheric 511 keV line.

Plotted in Figure 9 are the corrected 511 keV intensity profiles after subtraction of the estimated ~ 24 and ~ 47 day background variations determined from the profiles of the 680 keV feature and 5–8.5 MeV continuum. Data for “Earth-viewing” and “sky-viewing” geometries (see Fig. 4) are plotted at a resolution of ~ 24 days. Only data accumulated at cutoff rigidities > 4 GV and at times $> 10^4$ s from the last SAA traversal are included. Both sets of data exhibit a long-term build-up from production of a β^+ -unstable nucleus in the instrument. We have estimated the half-life of this isotope by assuming that the particle irradiation is proportional to the 680 keV time profile shown in Figure 8f. We obtain a half-life of 2.4 ± 0.3 yr for the “Earth-viewing” data and 2.1 ± 0.5 yr for the “sky-viewing” data, in reasonable agreement with ^{22}Na ($\tau_{1/2} = 2.6$ yr). The uncertainty in half-life for the “sky-viewing” data is larger because the fit to the data is not as good.

Clearly evident in the “sky-viewing” data plotted in Figure 9 is an increase each December when the Galactic center transited the aperture of the GRS. Only a hint of this increase is observed in the “Earth-viewing” data, as would be expected for a celestial source occulted by Earth (see Fig. 4). We have modeled the response of the GRS to discrete and diffuse celestial sources of γ -radiation. This procedure incorporates both the angular response of the GRS and the effects of occultation by the earth as determined at a resolution of 1 minute. The lines drawn through the data points in Figure 9 are the calculated GRS responses to a constant point source at the Galactic center (an extended source such as one proportional to the Galactic CO distribution yields almost the same response) superposed over a cubic function which mirrors the long-term build up of ^{22}Na in the instrument.

The derived intensities for a Galactic center source obtained from these fits are given in Table 1 under the classifications “sky viewing” and “Earth viewing” for magnetic rigidities > 4 GV. The errors given in the table are statistical and have been evaluated from the fits (N.B.: the “Earth viewing” and “Earth—sky viewing” uncertainties are probably underestimated because account has not been taken for the larger systematic variations in the data). The statistical significance for the detection of a Galactic 511 keV source covering the 7 yr observation is in excess of 30 standard deviations for the “sky-viewing” data! The inferred source intensity derived from the “Earth-viewing” data is consistent with the “sky-viewing” intensity, although at a much lower level of significance.

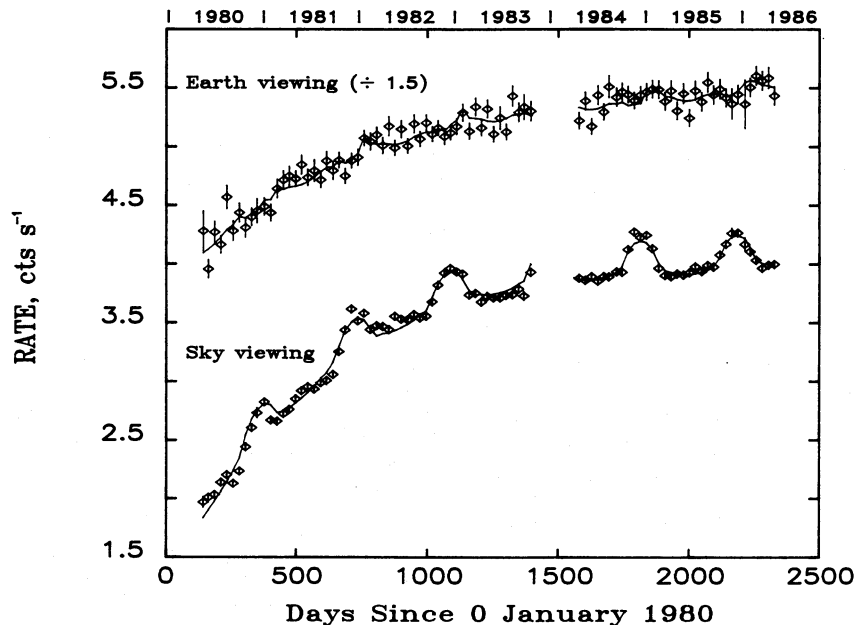


FIG. 9.—Time history of corrected 511 keV line measurements for “Earth-viewing” (N.B.: rate is divided by factor of 1.5 for purposes of plotting) and “sky-viewing” geometries. Data gap beginning in late 1983 occurred because *SMM*’s tape recorder was turned off during this period. Plotted lines are best-fit models incorporating the calculated response to a point source at the Galactic center superposed on a cubic function, which represents the build-up caused by production of ^{22}Na in the instrument.

d) Confirming the Celestial Origin

The striking difference between the profiles of the “sky-viewing” and “Earth-viewing” data plotted in Figure 9 is evidence for the celestial origin of the annual modulation observed in the “sky-viewing” data. If this modulation were due to some local background, we would expect it to be present in the “Earth-viewing” data at least at the same level. At the 99% confidence level, the largest amplitude for such an annual modulation allowable in the “Earth-viewing” data is $0.06 \text{ counts s}^{-1}$. This is about 20% of the level observed in the “sky-viewing” data. The above discussion assumes that the shape of any background modulation would be the same as in the “sky-viewing” data. In contrast, we showed in the previous

section that the “Earth-viewing” data actually exhibit weak evidence for the Galactic source occulted by Earth.

The celestial origin of the annual modulation can also be tested by determining whether it is dependent on background. The background in the annihilation line can be reduced by utilizing only data accumulated at vertical cut-off rigidities $> 11 \text{ GV}$. As can be seen in Table 1, the amplitude of the annual modulation for this restricted data set is not significantly different from what was obtained for the full set.

We are also able to demonstrate that the observed annual modulation is independent of the spectral fitting procedure. We did this by subtracting “sky-viewing” 3 day spectra from “Earth-viewing” spectra, as described in § IVc above. The residual spectrum (Fig. 6) then contains the atmospheric 511 keV line, its scattered continuum, an atmospheric bremsstrahlung continuum, and a negative contribution from any celestial source. The resulting 511 keV intensity profile was corrected for background in a similar manner to the data described above. A significant negative excursion was detected each December, as the Galactic center passed through the GRS aperture. This modulation was fitted by a model including a source at the Galactic center, the instrument’s aperture, and earth occultation. The resulting Galactic intensity is consistent with what was derived from the “sky-viewing” data (see Table 1).

A more detailed analysis utilizing the occultation of the proposed Galactic source by Earth provides compelling evidence for its celestial origin. A true celestial source is expected to exhibit characteristic time profiles in different viewing geometries relative to the earth. These profiles are illustrated in Figure 4 and discussed in § IIIb above. In order to illustrate the good agreement of the GRS data with the hypothesis that a Galactic source is the cause of the observed annual modulations, we have epoch-folded the data sets on an annual basis. The results of this folding procedure are plotted in Figure 10.

TABLE 1

FITS TO A GALACTIC SOURCE OF 511 keV RADIATION
A. ALL FIVE TRANSITS 1980–1986

Parameter	R	Peak Rate (counts s^{-1})
“Sky viewing”	$> 4 \text{ GV}$	0.309 ± 0.010
“Sky viewing”	$> 11 \text{ GV}$	0.293 ± 0.014
“Earth viewing”	$> 4 \text{ GV}$	0.410 ± 0.057
“Earth—sky viewing”	$> 4 \text{ GV}$	$0.361 \pm 0.019^*$

B. INDIVIDUAL TRANSITS ($R > 4 \text{ GV}$)

TRANSIT	PEAK RATE (count s^{-1})	
	“Sky Viewing”	“Earth—Sky Viewing”
1980/1981	0.295 ± 0.033	0.354 ± 0.038
1981/1982	0.308 ± 0.022	0.388 ± 0.033
1982/1983	0.346 ± 0.022	0.435 ± 0.036
1984/1985	0.386 ± 0.020	0.332 ± 0.039
1985/1986	0.267 ± 0.027	0.308 ± 0.042

* Sign of annual modulation reversed.

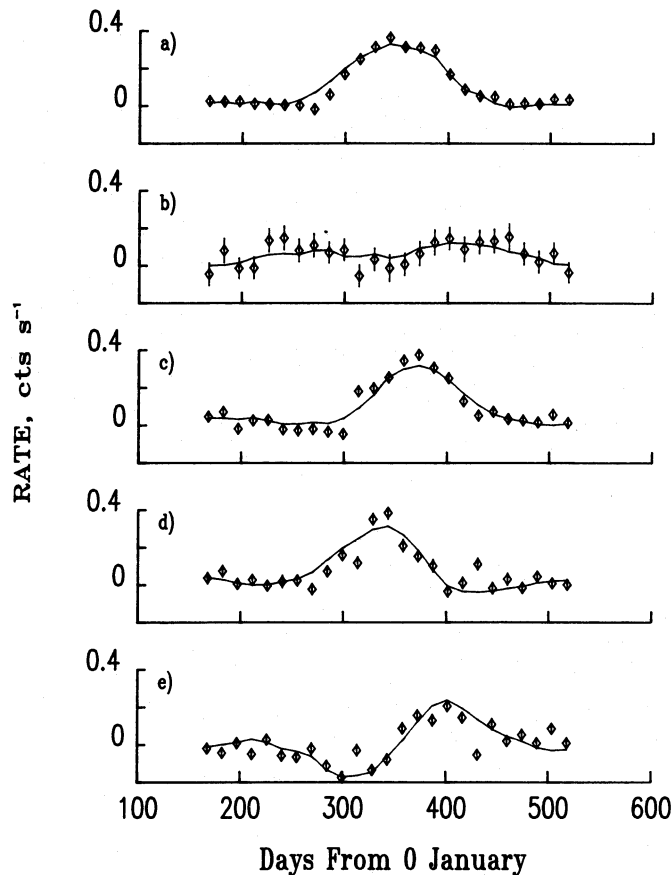


FIG. 10.—511 keV intensity measurements epoch-folded annually after correction for background and removal of long-term trends (e.g., build-up from ^{22}Na). The different viewing geometries are illustrated in Fig. 4: (a) “sky viewing,” (b) “Earth viewing,” (c) “partially occulted—early,” (d) partially occulted—late,” (e) fit to spectrum formed by first subtracting “partially occulted—late” data from “partially occulted—early” data. The curves represent the calculated response to an extended source proportional to the Galactic CO distribution. The amplitude of the response is normalized to the “sky-viewing” data in (a); there are no free parameters in (b), (c), (d), and (e).

The calculated time profile for an extended source proportional to the distribution of Galactic CO (Leising and Clayton 1985), including the angular response of the GRS and the occultation of the source by Earth, are shown by the curves in the figure. The shape of the plotted curves are entirely determined by the calculation. The only free parameter is the amplitude of the celestial signal. This amplitude was determined by fitting the model to the “sky-viewing” data in Figure 10a. This amplitude was then used in plotting the remaining calculated profiles in the figure.

It is clear that the epoch-folded data support the hypothesis that a celestial source of 511 keV radiation has been detected by the GRS experiment on *SMM*. There are some minor excursions of the data from the model, however. In Figure 10a, the model does not fit the rising edge of the annual increase. This is due to the fact that the cubic function used to fit the long-term increase in the 511 keV background does only a fair job during the first few years of the mission (see Fig. 9). A few of the data points also exhibit some large excursions which we attribute to residual systematic variations due to orbital precession. On the whole, the data follow the model curves remarkably well. The early occultation of the source is clearly

seen in data accumulated with Earth off to the left side of *SMM* (Fig. 10c), as viewed from the North Pole (see Fig. 4). The late occultation is seen in data accumulated with the earth to the right (Fig. 10d). This occultation effect is also clearly revealed in Figure 10e which shows the fitted 511 keV intensity after first subtracting the spectra accumulated in Figure 10c from those in Figure 10d. The subtracted spectrum on which these fits were made no longer contained the radioactive background lines. This separate fit was performed in order to demonstrate that the final results were once again independent of spectral shape.

Similarity of the time profiles of the 511 keV line and the 1.81 MeV Galactic ^{26}Al line detected by *SMM* (Share *et al.* 1985) provide further evidence for the celestial origin of the annihilation line. This is demonstrated in Figure 11 where epoch-folded ^{26}Al intensities are compared with the 511 keV profile derived from the data in Figure 11. The agreement is excellent and also indicates that the centroid of the 511 keV source distribution lies within about 25° of the Galactic center (Share *et al.* 1985). Work is underway both to determine this position with greater precision and to set limits on the spatial extent of the annihilation radiation source. The slightly broader ^{26}Al distribution is probably due to the larger effective aperture of the *SMM* spectrometer at higher energies and not to any measurable differences in the spatial distributions of the lines.

We conclude that the increase in intensity of the 511 keV line each December is due to a celestial source located in the general vicinity of the Galactic center.

e) Year-to-Year Variability

The overall statistical significance ($> 30 \sigma$) of this detection of Galactic annihilation radiation permits us to measure any year-to-year variability of the emission. This study was done using the 511 keV intensities derived from both the “sky-viewing” spectra and from the “Earth minus sky-viewing” difference spectra. In obtaining the yearly intensities we fitted each transit separately, using the calculated response to a Galactic center source and a polynomial representation for the time variation of the background observed between transits. The parameters of this polynomial background were allowed to vary from transit to transit in order to provide the best overall fit to the “sky-viewing” data. This was done because the best-fit cubic function used to fit the build-up in background over the entire 7 yr period did not adequately describe the background variations observed during the first 2 years of the mission (see Fig. 9). Because the background level of the “Earth minus sky-viewing” intensity profile did not vary significantly between transits over the mission, we used a constant to represent the background for each transit.

The results of this analysis are summarized in Table 1. As mentioned above, the errors quoted are statistical; due to the larger systematic variations in the “Earth—sky viewing” data the true uncertainties may also be larger than listed. The intensities derived using the two sets of data are in reasonable agreement with one another. Within each data set the root mean square of the deviations is less than 14% of the mean value. The most striking difference in the measured values for the “sky-viewing” data, about 35% of the mean value, occurred between the last two transits. However, this is not likely to be due to variability of the source because the percentage variation in flux measured in the “Earth minus sky-viewing” data over the same time period was less than 10%. From this dis-

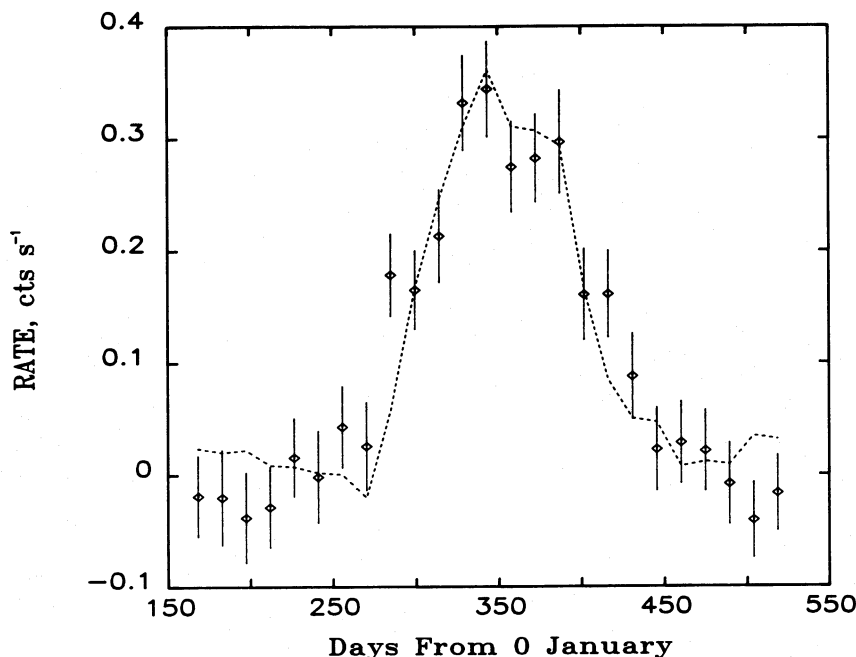


FIG. 11.—Epoch-folded intensities (sky-viewing) of the 1.81 MeV ^{26}Al line measured over the same 6 yr period by *SMM* are compared with the 511 keV profile (dashed curve) representing the data plotted in Fig. 8a. The 1.81 MeV intensities are normalized to the 511 keV rates.

cussion, we conclude that the maximum year-to-year variability in line intensity is less than about 30%.

f) 511 keV Line Flux

In this section we discuss the determination of the incident flux of 511 keV photons for two scenarios: (1) a point source at the Galactic center and (2) a distributed Galactic source. There are two corrections which must first be applied to the peak rates listed in Table 1 in order to estimate the flux in the line. These corrections are due to the effects of a positronium continuum and a Galactic 5–8.5 MeV continuum on our corrected 511 keV rates. As we show below these effects are each on the order of 20% and cancel each other.

If the Galactic annihilation line is accompanied by a significant contribution from a positronium continuum, then its measured intensity may be overestimated (Ramaty and Lingenfelter 1987; Leventhal 1986). This is true for moderate resolution instruments like the GRS because some fraction of the positronium continuum may be integrated under the Gaussian used to fit the 511 keV line. We have calculated the contribution that such a positronium continuum (Ore and Powell 1949) makes to our fitted 511 keV line intensity under the assumption that 90% of the positrons annihilate via the formation of positronium (Brown, Leventhal, and Mills 1986). This was done by first adding a 511 keV line, with an intensity comparable to that observed from the Galaxy, to the background spectrum (Fig. 5) and then fitting the data using our standard technique (§ IIIc). We then added both a 511 keV line and positronium continuum, with the correct relative intensities, to the background spectrum and once again fit the data. When the positronium continuum is added to the spectrum, the measured line intensity increases by about 20%. Thus, for a 90% positronium fraction, we must reduce our measured 511 keV line intensities by about 20%.

As noted earlier, we have used the 5–8.5 MeV continuum

band in order to correct systematic variations in our measurements of the 511 keV line intensities. This was done by subtracting a fraction of the intensity profile of the 5–8.5 MeV continuum from the 511 keV profile. For this reason any Galactic continuum radiation present in the GRS spectrum would cause us to underestimate the Galactic 511 keV flux. Measurements of the Galactic continuum have been summarized by Lavigne *et al.* (1986). We estimate from these measurements that, in correcting our 511 keV time histories, we have also subtracted off between 15% and 30% of the Galactic intensity. Analysis of the 511 keV intensity profile prior to correcting for the ~ 24 and 47 day modulations yields results which are consistent with this conclusion.

An additional systematic effect that could artificially increase the Galactic 511 keV flux measured by *SMM* has been suggested by Leventhal (1986). He suggests that Galactic photons > 1 MeV produce electron-positron pairs in the detector, satellite, or Earth's atmosphere resulting in a significant increase in annihilation photons which are then detected in addition to the Galactic 511 keV photons. The total flux of Galactic photons with energies > 1 MeV can be estimated from the summary of data given in Lavigne *et al.* (1986). We estimate that the integral flux > 1 MeV is about twice the observed Galactic 511 keV line flux observed by *SMM*.

We first used a Monte Carlo algorithm (Kinzer *et al.* 1979) to estimate the fraction of this high-energy Galactic emission that can interact in the instrument and produce detectable 511 keV radiation. Under the assumption that the shields of the detector were not operating, only about 2% of the high-energy Galactic photons would contribute to the observed Galactic 511 keV line. For shields with energy loss thresholds of a few hundred keV, $< 0.1\%$ of the high-energy photons would appear in the line. This effect is therefore negligible.

Another Monte Carlo calculation was performed (Jung 1987) to determine the fraction of > 1 MeV Galactic γ -rays

which interact in the earth's atmosphere and produce albedo 511 keV photons. This calculation shows that about one 511 keV photon will be produced which leaves Earth's atmosphere for each five Galactic photons > 1 MeV which are incident on the atmosphere. This could account for about 40% of our measured Galactic 511 keV intensity. However, only about 5%–10% of these atmospheric photons will penetrate the anti-coincidence shielding of the detector in the "sky-viewing" geometry; therefore we estimate that high-energy Galactic photons can produce for no more than about 5% of our measured 511 keV flux from the Galaxy. As we discuss below, the actual contribution is considerably less than this.

Data plotted in Figure 9 demonstrate, convincingly, that any effects due to the production of albedo 511 keV γ -rays by high-energy Galactic photons are negligible. If such a process played a significant role in the annual increases shown in the "sky-viewing" data, it should have produced even more significant increases centered about 6 months later in the "Earth-viewing" data. This is true because at that time high-energy radiation from the Galactic center region is incident on the rear of the detector and any 511 keV radiation produced in the atmosphere can enter the GRS's aperture directly without passing through the shielding. It is clear that no such increases were observed.

From the above discussion we conclude that our best estimate of the Galactic annihilation line flux is derived directly from the measured rates given in Table 1, and that any corrections either approximately cancel one or another or are negligible. However, due to these corrections, the uncertainty in the flux is clearly dominated by systematics rather than statistics. Based on the uncertainties in the corrections for the positronium continuum and for the background subtractions using the 5–8.5 MeV data, we feel that a conservative estimate of this systematic uncertainty is about $\pm 20\%$. If the radiation originates from a point source at the Galactic center, its time-averaged flux is $(2.1 \pm 0.4) \times 10^{-3} \gamma \text{ cm}^{-2} \text{ s}^{-1}$. For a distributed source proportional to the concentration of CO in the Galaxy (Leising and Clayton 1985), the *SMM* observations require a flux of $(1.6 \pm 0.3) \times 10^{-3} \gamma \text{ cm}^{-2} \text{ s}^{-1} \text{ rad}^{-1}$ at the Galactic center.

V. DISCUSSION

a) Observations

The gamma-ray spectrometer on NASA's *Solar Maximum Mission* satellite has detected an intense source of annihilation radiation emanating from the vicinity of the Galactic center. The 511 keV annihilation line was detected from about mid-October to mid-February in each of 5 yr from 1980 to 1986 (no measurement was made during the 1983/1984 transit because the satellite's tape recorder was turned off). We have conducted a variety of tests which confirm the celestial origin of the emission. These tests include utilization of low-background data, occultation of the source by Earth, and comparison of the 511 keV measurement with the earlier *SMM* detection of the 1.81 MeV line from ^{26}Al (Share *et al.* 1985), where observational problems differ markedly.

The statistical significance of the overall detection of the Galactic 511 keV line exceeds 30σ . There is no evidence for any variability in intensity of the source; the maximum year-to-year variation is less than 30%. If the emission came from a point source at the Galactic center, its flux would be $(2.1 \pm 0.4) \times 10^{-3} \gamma \text{ cm}^{-2} \text{ s}^{-1}$ (the uncertainty in flux is domi-

nated by systematics). However, as we discuss below, it is not likely that a single source at the center can account for this high intensity.

These new *SMM* observations are compared with previous measurements of the 511 keV line in Figure 12. The plotted *SMM* data points were derived from the values given in Table 1 assuming a point source at the Galactic center. There were three balloon-borne experiments performed while the *SMM* spectrometer was observing the vicinity of the Galactic center. All of them utilized high-resolution germanium spectrometers with apertures of about 15° FWHM. Two of the observations were made by the same Bell/Sandia instrument (Leventhal *et al.* 1986) that detected the Galactic center source in 1977 and 1979; the third measurement was performed by an experiment prepared by the GSFC/CENS collaboration (Paciesas *et al.* 1982). No evidence was found for the presence of the Galactic center annihilation line that had been observed prior to 1980 (the limits plotted are at the 98% confidence level). The *HEAO 3* observations bracket the time interval when the source of the annihilation radiation apparently changed in emissivity.

There is a clear disparity between the *SMM* observations and the three contemporaneous balloon-borne measurements if one assumes that the emission comes from a point source at the Galactic center. One possible explanation is that the source is highly variable on time scales of days to weeks. This possibility can be studied by inspection of Figure 13, which plots 3 day accumulations of 511 keV line measurements by *SMM* during the 1981/1982 and 1984/1985 transits of the Galactic center. Systematic background variations have been corrected for using the technique described in § IVc. Residual systematic background variations are more evident in the 1981/1982 transit due to the unstable pointing of *SMM* and lack of aspect information from late 1980 to early 1984. During this time period, the satellite could have been pointed up to about 11° from the Sun; this uncertainty results in our incorrectly binning data relative to the atmospheric albedo. From the 1984/1985 transit, it is clear that any intrinsic source variability on time scales of days is no greater than about 30%. Furthermore, there is no evidence for a decrease in excess of about 30% in the 511 keV flux measured by the *SMM*/GRS at the time of the balloon experiments.

The upper limits from the recent balloon-borne experiments can be reconciled with the *SMM* measurements if one assumes that the bulk of the emission comes from a distributed source. In this case, only a fraction of the flux observed by *SMM* would be detected by instruments with fields of view of 15° FWHM. If we assume that the Galactic 511 keV line emission comes from regions of current star formation, then its intensity profile should be proportional to the CO distribution in the Galaxy (Leising and Clayton 1985). For such a distribution, the *SMM* measurements require a flux of $(1.6 \pm 0.3) \times 10^{-3} \gamma \text{ cm}^{-2} \text{ s}^{-1} \text{ rad}^{-1}$ (error is dominated by systematic uncertainties) at the Galactic center. We have estimated the response of all the experiments exhibited in Figure 12 to such a spatial distribution of γ -rays, using their measured instrument response functions (e.g., see Mahoney *et al.* 1981). These estimates were made by folding the normalized CO distribution through the respective angular response functions of the experiments. For the Rice measurements, we have also applied corrections to account for the contribution that a 90% positronium fraction would make to the observed line intensities. The dashed horizontal lines give our estimates of the intensities, in $\gamma \text{ cm}^{-2} \text{ s}^{-1}$, that the different experiments would have reported

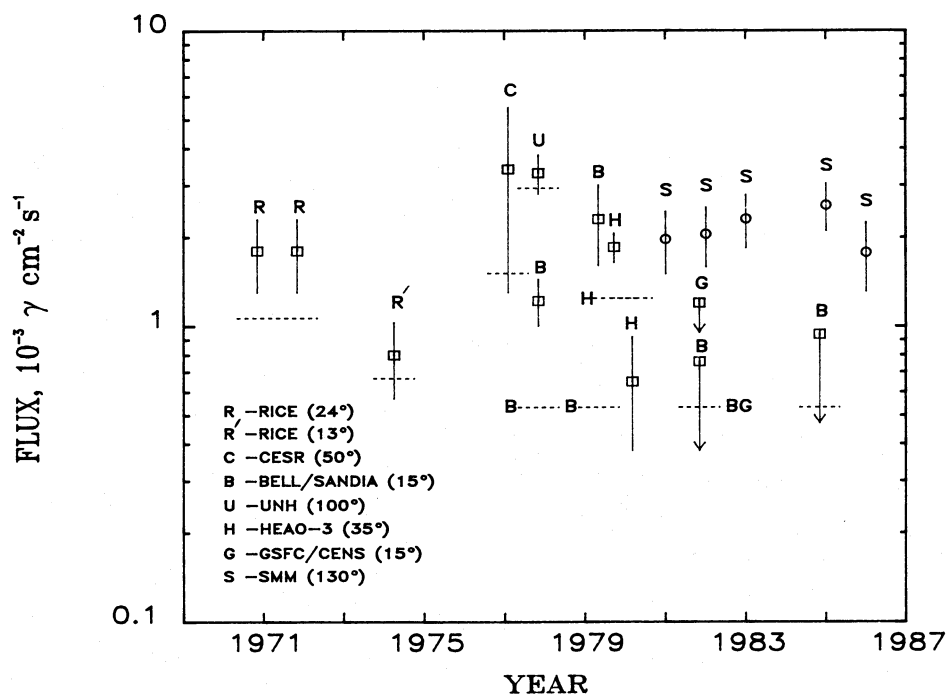


FIG. 12.—History of Galactic center 511 keV line measurements. Dashed horizontal lines are estimates of the contribution to measured intensities from a distributed source proportional to Galactic CO, normalized to a flux of $1.6 \times 10^{-3} \gamma \text{ cm}^{-2} \text{ s}^{-1} \text{ rad}^{-1}$ at the center. References for the measurements are Rice (Johnson and Haymes 1973), CESR (Alberhe *et al.* 1981), UNH (Gardner *et al.* 1982), B/S (Leventhal *et al.* 1978, 1986), HEAO 3 (Riegler *et al.* 1981), GSFC/CENS (Paciesas *et al.* 1982).

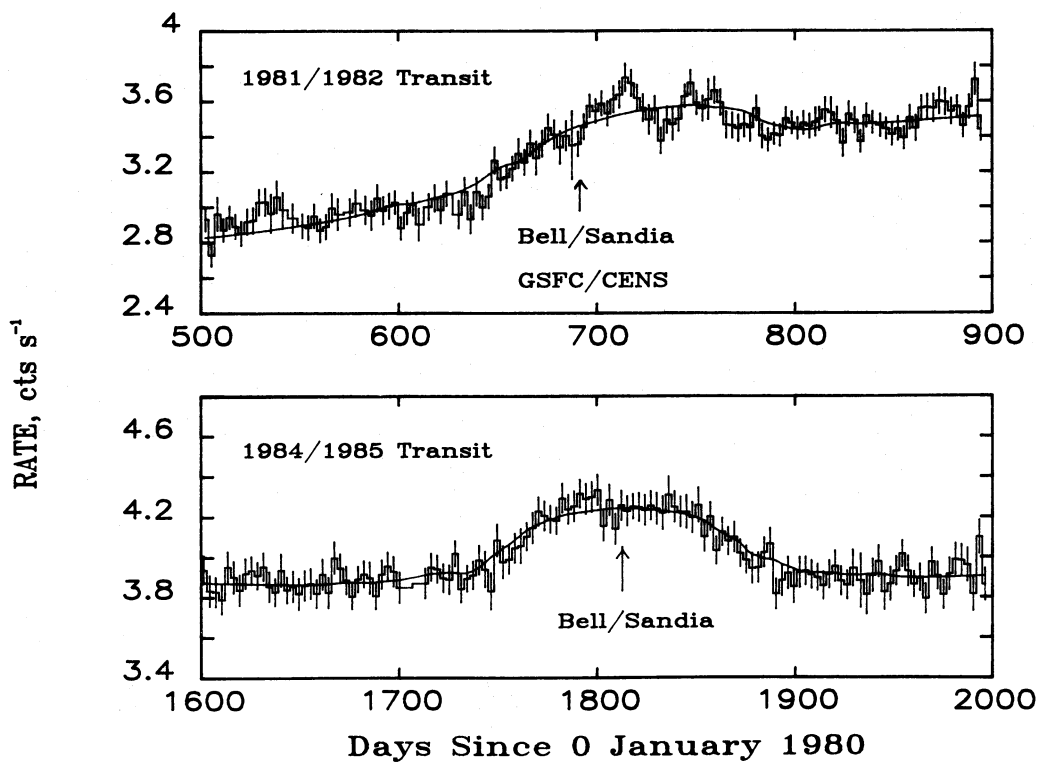


FIG. 13.—Time history of SMM 511 keV line measurements at 3 day resolution from “sky-viewing” data accumulated >4 GV during the 1981/1982 and 1984/1985 Galactic center transits. Residual systematic background variations are more noticeable in the earlier transit (see text). The line drawn through the data is the model used in Fig. 9. The arrows denote the times of the Bell/Sandia and GSFC/CENS balloon-borne observations.

for such a diffuse source of 511 keV line radiation. Note that the uncertainty in these estimates is about 20%, reflecting the systematic uncertainty in the flux observed by SMM.

Both the Bell/Sandia and GSFC/CENS experiments would have measured an intensity of about $5 \times 10^{-4} \gamma \text{ cm}^{-2} \text{ s}^{-1}$ from this diffuse 511 keV emission. This flux is consistent with the limits set by these experiments subsequent to 1980. A diffuse 511 keV source can also account for much, if not all, of the observed line intensities measured by the Rice, CESR, and UNH experiments. In fact, Haymes *et al.* (1975) suggested that the lower intensity observed in 1974 might have been due to the reduced field of view (13° FWHM vs. 24° in 1970) of the experiment and an extended 511 keV source. We have plotted the CENS flux derived using their detailed analysis of a source traversing the aperture of the telescope.

Most summaries of 511 keV line observations have quoted the value $4.0 \times 10^{-3} \gamma \text{ cm}^{-2} \text{ s}^{-1}$ for the UNH observation (Gardner *et al.* 1982); however, these authors point out that the line flux is dependent on the positronium fraction. For the 90% positronium fraction assumed in this work, the UNH flux is about $3.2 \times 10^{-3} \gamma \text{ cm}^{-2} \text{ s}^{-1}$. This is the value plotted in Figure 12; it is in good agreement with what we estimate that experiment would have observed from the diffuse source. (Note that the plotted "point-source" intensities observed by SMM are smaller than our estimate of the UNH spectrometer's response to the diffuse 511 keV flux. This appears to be contradictory because SMM's aperture is larger; however, the SMM "point source" intensities were derived from a difference of Galactic center and anticenter exposures. Because there is significant 511 keV emission in the anticenter direction for a CO distribution, the SMM points only reflect the excess intensity from the galactic center and not its absolute value. On the other hand, the UNH background measurements were made at high Galactic latitudes where any contribution from the diffuse emission would be small.)

The diffuse 511 keV contribution only partially accounts for the line intensities measured by the Bell/Sandia experiment in 1977 and 1979. The excess intensities over the diffuse contribution inferred from these observations are (0.7 ± 0.2) and $(1.9 \pm 0.7) \times 10^{-3} \gamma \text{ cm}^{-2} \text{ s}^{-1}$, respectively. It is important to note that the significance of any point source contribution has been weakened by the presence of diffuse Galactic emission. On the other hand, the presence of a point source with an intensity of $\sim 0.5\text{--}1.0 \times 10^{-3} \gamma \text{ cm}^{-2} \text{ s}^{-1}$ prior to 1980 is not inconsistent with any of the pre-1980 balloon measurements.

We estimate that the HEAO 3 spectrometer would have detected an equivalent flux in its aperture of about $1.25 \times 10^{-3} \gamma \text{ cm}^{-2} \text{ s}^{-1}$ in both its 1979 autumn and 1980 spring exposures to the diffuse Galactic radiation. The autumn observation exceeds this value by over 2σ , while the spring observation is over 2σ low (Riegler *et al.* 1981). This change in intensity appears to confirm, the disappearance of the source observed by the Bell/Sandia experiment prior to 1980. However, the spring observation is marginally inconsistent with our conclusion that a bulk of the 511 keV radiation observed by SMM is emitted by a diffuse Galactic source. Such a diffuse source could not exhibit variability on these time scales. We have no explanation for this. We note that the new SMM observations support earlier contentions that a bulk of the annihilation radiation came from a diffuse source (Alberhe *et al.* 1981; Dunphy, Chupp, and Forrest 1983).

A diffuse origin is also in conflict with the statement in Riegler *et al.* (1981) that the HEAO 3 "data rule out most

extended models for positron production, such as by cosmic-ray interactions in the interstellar medium or by distributions of many supernovae, novae, or pulsars." In reviewing the HEAO 3 measurements, we feel that this latter statement is too strong. A CO distribution fits the Fall HEAO-3 observations only marginally worse ($\chi^2/\text{DOF} = 1.45$) than the best-fit distribution ($\chi^2/\text{DOF} = 1.34$) described by Riegler *et al.*, which is somewhat broader than a point source.

In summary we conclude that the SMM measurements, when compared with earlier observations, suggest the presence of an intense flux of annihilation radiation distributed relatively broadly along the Galactic plane. When such a diffuse contribution to the other Galactic 511 keV observations is taken into account, the evidence for a time variable source at the Galactic center is weakened.

b) Galactic Sources of Positrons

A diffuse glow of annihilation radiation is expected because of the $\sim 10^5$ yr lifetime of positrons in interstellar space (Colgate 1970; Ramaty and Lingenfelter 1981). This glow is similar to that observed at 1.809 MeV due to the accumulation of ^{26}Al in the interstellar medium (Mahoney *et al.* 1984; Share *et al.* 1985). There are many Galactic sources which can provide the positrons. These include stars expelling radioactive nuclei produced by nucleosynthesis (Ramaty, Kozlovsky, and Lingenfelter 1979; Ramaty and Lingenfelter 1981), cosmic-ray interactions with the interstellar medium (Kozlovsky, Lingenfelter, and Ramaty 1987), pulsars (Sturrock 1971), and stellar flares.

The most plausible sources of the radioactive isotopes are supernovae, novae, red giants, and Wolf-Rayet stars. All of these have been suggested as sources for the interstellar ^{26}Al observed by HEAO 3 and SMM. ^{26}Al decays 82% of the time with the emission of a positron. If we assume that 90% of the positrons annihilate through the formation of positronium, then we would expect the flux of 511 keV photons to be about 55% of the observed flux of 1.809 MeV photons, i.e., about $2.5 \times 10^{-4} \gamma \text{ cm}^{-2} \text{ s}^{-1} \text{ rad}^{-1}$. This accounts for only about 15% of the observed 511 keV intensity.

^{26}Al is not expected to be the most plentiful positron emitter produced by nucleosynthesis. Only $3 M_\odot$ of ^{26}Al are estimated to be distributed in our Galaxy at the present time, based on the gamma-ray observations (Mahoney *et al.* 1984). On the other hand, a few tenths of a M_\odot of ^{56}Ni may be produced in a single supernova. The ^{56}Ni decays into ^{56}Co , which in turn decays 19% of the time with the emission of a positron. If the rate of Galactic supernovae is about 1 every 100 yr, then more than $1000 M_\odot$ of ^{56}Co can be produced during the $\sim 10^6$ yr lifetime of the ^{26}Al . If all the positrons from the ^{56}Co decays were able to escape from the source, this would result in a continuous flux in excess of $\sim 10^{-2} \gamma \text{ cm}^{-2} \text{ s}^{-1} \text{ rad}^{-1}$ at 511 keV. However, it is not known what fraction of the positrons actually can leave the supernova shell; this is dependent on the geometry and magnetic fields. This fraction could be as large as 10% (Colgate 1970); therefore ^{56}Ni produced in supernovae could account for as much as about 50% of the observed flux of Galactic 511 keV radiation.

Another radioactive product of nucleosynthesis in supernovae is ^{44}Ti . It decays into ^{44}Sc with a half-life of 48 yr via electron capture. The ^{44}Sc decays via positron emission into ^{44}Ca . Calculations indicate that 10^{-4} to $10^{-2} M_\odot$ of ^{44}Ti can be produced in supernovae (Nomoto, Thielemann, and Yokoi 1984; Woosley, Taam, and Weaver 1986) which suggests that

from 1 to 100 M_{\odot} of ^{44}Ti are produced during the 10^6 yr lifetime of ^{26}Al . Therefore ^{44}Ti can produce a flux of between about 10^{-4} and 10^{-2} γ cm^{-2} s^{-1} rad^{-1} in the 511 keV line.

Novae may produce significant quantities of ^{22}Na , which decays ($\tau_{1/2} = 2.6$ yr) with the emission of a positron. If no more than $2 \times 10^{-7} M_{\odot}$ of ^{22}Na is produced during a nova rich in Ne and if the Galactic rate of these novae is about 10 per year, then the resulting 511 keV flux is no more than about 2% of the observed Galactic intensity. This is about a factor of 2 below the contribution that is expected from positrons produced by charged particle interactions in the interstellar medium (Ramaty and Lingenfelter 1981).

We wish to thank Steve Matz for adapting the UCSD Monte Carlo code, provided to us by Greg Jung, to the

SMM/GRS geometry. Our thanks also go to Mark Leising for assisting in estimating the SMM response to different source models, for suggesting that ^{44}Ti could provide a significant source of interstellar positrons (Stan Woosley suggested this independently), and for stimulating discussions. Neil Johnson and Mark Strickman prepared some of the computer algorithms used in this analysis. Discussions with Jim Adams helped us to understand some of the systematic variations caused by particle irradiation in the SAA. We also wish to thank Reuven Ramaty, Marvin Leventhal, and William Mahoney for their suggestions concerning this work. Tom Rotelli provided important support in the early phases of this work. This work was supported by NASA contract S-14513-D at NRL and grant NAS 5-28609 at UNH, and by BMFT contract 010k 017-za/ws/wrk 0275:4 at MPE.

REFERENCES

- Alberhe, F., Leborgne, J. F., Vedrenne, G., Boclet, D., Durouchoux, P., and da Costa, J. M. 1981, *Astr. Ap.*, **94**, 214.
 Brown, B. L., Leventhal, M., and Mills, A. P., Jr. 1986, *Phys. Rev. A.*, **33**, 2281.
 Colgate, S. A. 1970, *Ap. Space Sci.*, **8**, 457.
 Dunphy, P. P., Chupp, E. L., and Forrest, D. J. 1983, in *Positron-Electron Pairs in Astrophysics*, ed. M. L. Burns, A. K. Harding, and R. Ramaty (AIP Conference Proceedings 101), (New York: AIP), p. 237.
 Forrest, D. J., et al. 1980, *Solar Phys.*, **65**, 15.
 Gardner, B. M., Forrest, D. J., Dunphy, P. P., and Chupp, E. L. 1982, in *The Galactic Center*, ed. G. R. Riegler and R. D. Blanford (AIP Conference Proceedings 83) (New York: AIP), p. 144.
 Geldzahler, B. J., Share, G. H., Kinzer, R. L., Forrest, D. J., Chupp, E. L., and Rieger, E. 1985, *Proc. 19th Int. Cosmic Ray Conf.*, La Jolla (NASA CP-2376), **1**, 187.
 Haymes, R. C., Walraven, G. D., Meegan, C. A., Hall, R. D., Djuth, F. T., and Shelton, D. H. 1975, *Ap. J.*, **201**, 593.
 Humble, J. E., Smart, D. F., and Shea, M. A. 1979, *Proc. 16th Int. Cosmic Ray Conf.*, Kyoto, **4**, 303.
 Johnson, W. N., III, and Haymes, R. C. 1973, *Ap. J.*, **184**, 103.
 Jung, G. 1987, private communication.
 Jung, G., and Matz, S. M. 1987, private communication.
 Kozlovsky, B., Lingenfelter, R. E., and Ramaty, R. 1987, *Ap. J.*, **316**, 801.
 Lavigne, J. M., Mandrou, P., Neil, M., Agrinier, B., Bonfand, E. and Parlier, B. 1986, *Ap. J.*, **308**, 370.
 Leising, M. D., and Clayton, D. D. 1985, *Ap. J.*, **294**, 591.
 Leising, M. D., Share, G. H., Kinzer, R. L., Chupp, E. L., Forrest, D. J. and Rieger, E. 1988, *Ap. J.*, in press.
 Letaw, J. R., Share, G. H., Kinzer, R. L., Silberberg, R., Chupp, E. L., Forrest, D. J., and Rieger, E. 1986, *Adv. Space Res.*, **6**, 133.
 ———. 1987, *J. Geophys. Res.*, submitted.
 Leventhal, M. 1986, private communication.
 Leventhal, M., MacCallum, C. J., Hutera, A. F., and Stang, P. D. 1980, *Ap. J.*, **240**, 338.
 Leventhal, M., MacCallum, C. J., Hutera, A. F., and Stang, P. D. 1986, *Ap. J.*, **302**, 459.
 Leventhal, M., MacCallum, C. J., and Stang, P. D. 1978, *Ap. J. (Letters)*, **225**, L11.
 Mahoney, W. A., Ling, J. C., and Jacobson, A. S. 1981, *J. Geophys. Res.*, **86**, 11098.
 Mahoney, W. A., Ling, J. C., Wheaton, W. A., and Jacobson, A. S. 1984, *Ap. J.*, **286**, 578.
 Nomoto, K., Thielemann, F.-K., and Yokoi, K. 1984, *Ap. J.*, **286**, 644.
 Ore, A., and Powell, J. L. 1949, *Phys. Rev.*, **75**, 1696.
 Paciasas, W. S., Cline, T. L., Teegarden, B. J., Tueller, J., Durouchoux, P., and Hameury, J. M. 1982, *Ap. J. (Letters)*, **260**, L7.
 Ramaty, R., Kozlovsky, B., and Lingenfelter, R. E. 1979, *Ap. J. Suppl.*, **40**, 487.
 Ramaty, R., and Lingenfelter, R. E. 1981, *Phil. Trans. R. Soc. London, A*, **301**, 671.
 ———. 1987, in *The Galactic Center*, ed. D. C. Backer (AIP Conference Proceedings 155) (New York: AIP), p. 51.
 Riegler, G. R., Ling, J. C., Mahoney, W. A., Wheaton, W. A., Willett, J. B., Jacobson, A. S., and Prince, T. A. 1981, *Ap. J. (Letters)*, **248**, L13.
 Share, G. H., Forrest, D. J., Chupp, E. L., and Rieger, E. 1983, in *Positron-Electron Pairs in Astrophysics*, ed. M. L. Burns, A. K. Harding, and R. Ramaty (AIP Conference Proceedings 101) (New York: AIP), p. 15.
 Share, G. H., Kinzer, R. L., Kurfess, J. D., Forrest, D. J., Chupp, E. L., and Rieger, E. 1985, *Ap. J. (Letters)*, **292**, L61.
 Share, G. H., Kinzer, R. L., Messina, D. C., Purcell, W. R., Chupp, E. L., Forrest, D. J., and Reppin, C. 1987, *Proc. 20th Int. Cosmic Ray Conf.*, Moscow, **1**, 156.
 Share, G. H., Kinzer, R. L., Messina, D. C., Purcell, W. R., Chupp, E. L., Forrest, D. J., and Rieger, E. 1986, *Adv. Space Res.*, **6**, 145.
 Sturrock, P. A. 1971, *Ap. J.*, **164**, 529.
 Woosley, S. E., Taam, R. E., and Weaver, T. A. 1986, *Ap. J.*, **301**, 601.

EDWARD L. CHUPP and DAVID J. FORREST: Physics Department, University of New Hampshire, Durham, NH 03824

ROBERT L. KINZER: Code 4153, Naval Research Laboratory, Washington, DC 20375-5000

JAMES D. KURFESS: Code 4150, Naval Research Laboratory, Washington, DC 20375-5000

DANIEL C. MESSINA AND GERALD H. SHARE: Code 4152, Naval Research Laboratory, Washington, DC 20375-5000

WILLIAM R. PURCELL: Code 4151, Naval Research Laboratory, Washington, DC 20375-5000

CLAUS REPPIN: Max-Planck-Institut für Physik und Astrophysik, Institute für extraterrestrische Physik, 8046 Garching bei München, Federal Republic of Germany